Travel-Time and Amplitude Sensitivity Kernels

Emmanuel Skarsoulis
Foundation for Research and Technology Hellas
Institute of Applied and Computational Mathematics
P.O. Box 1385, GR-71110 Heraklion, Greece
phone: +30-2810-391776 fax: +30-2810-391801
email: eskars@iacm.forth.gr

in collaboration with
Bruce Cornuelle and Matthew Dzieciuch
Scripps Institution of Oceanography
University of California, San Diego
La Jolla, CA 92093-0225
phone: (858) 534-4021 fax: (858) 534-9820
email: bdc@ucsd.edu, mad@uscd.edu

Award Number: N00014-11-1-0186
http://www.iacm.forth.gr, http://sio.ucsd.edu

LONG-TERM GOALS

Our long-term goal is to study the sensitivity behavior of travel-time and arrival-amplitude observables due to sound-speed perturbations in low-frequency, long-range acoustic propagation in the ocean.

OBJECTIVES

The leading objective of this project is to rigorously study the asymptotic behavior of wave-theoretic travel-time sensitivity kernels with increasing range, as a means to explain their observed convergence towards the corresponding ray-theoretic sensitivity kernels even at low frequencies. Further objectives include the derivation and study of 2D and 3D first-order amplitude sensitivity kernels, as well as vertical sensitivity kernels for arrival amplitudes, first- and second-order. A last objective is the study of sensitivity behavior of late arrivals depending on propagation frequency and range.

APPROACH

Previous work has revealed a numerical convergence of wave-theoretic travel-time vertical sensitivity kernels (VTSKs) towards the corresponding ray-theoretic sensitivity kernels with increasing range even at low frequencies [1]. To study this behavior, the asymptotic form of finite-frequency kernels with increasing range is rigorously derived here using a stationary-phase approach [2]. The wave-theoretic VTSK involves an integral over frequency with a rapidly oscillating kernel, the oscillation rate increasing with propagation range. The stationary-phase approach is used to evaluate the asymptotic form of this integral and finally of the VTSK for long ranges.

Report Documentation Page

Form Approved
OMB No. 0704-0188

1. REPORT DATE	2. REPORT TYPE	3. DATES COVERED
SEP 2011		**00-00-2011 to 00-00-2011**

4. TITLE AND SUBTITLE	5a. CONTRACT NUMBER
Travel-Time and Amplitude Sensitivity Kernels	5b. GRANT NUMBER
	5c. PROGRAM ELEMENT NUMBER
6. AUTHOR(S)	5d. PROJECT NUMBER
	5e. TASK NUMBER
	5f. WORK UNIT NUMBER
7. PERFORMING ORGANIZATION NAME(S) AND ADDRESS(ES) **Foundation for Research and Technology Hellas,Institute of Applied and Computational Mathematics,PO Box 1385,GR-71110 Heraklion, Greece,**	8. PERFORMING ORGANIZATION REPORT NUMBER
9. SPONSORING/MONITORING AGENCY NAME(S) AND ADDRESS(ES)	10. SPONSOR/MONITOR'S ACRONYM(S)
	11. SPONSOR/MONITOR'S REPORT NUMBER(S)

12. DISTRIBUTION/AVAILABILITY STATEMENT
Approved for public release; distribution unlimited

13. SUPPLEMENTARY NOTES

14. ABSTRACT

15. SUBJECT TERMS

16. SECURITY CLASSIFICATION OF:			17. LIMITATION OF ABSTRACT	18. NUMBER OF PAGES	19a. NAME OF RESPONSIBLE PERSON
a. REPORT	b. ABSTRACT	c. THIS PAGE			
unclassified	**unclassified**	**unclassified**	**Same as Report (SAR)**	**12**	

The derivation of 2D and 3D first-order amplitude sensitivity kernels relies on the first Born approximation for perturbations of the Green's function. The vertical sensitivity kernels of arrival amplitudes – first and second order – are derived from perturbations of the range-independent Green's function and normal-mode theory. Two alternative definitions for arrival amplitude perturbations are considered – perturbation of arrival maximum and perturbation of arrival amplitude at fixed time.

WORK COMPLETED

The project was initiated in February 2011. Up to the present (September 2011) the asymptotic study of the wave-theoretic travel-time vertical sensitivity kernel has been completed, as well as the derivation and study of 2D and 3D amplitude sensitivity kernels, and first/second-order vertical sensitivity kernels of arrival amplitudes. The study of the sensitivity behavior of late arrivals has been initiated.

RESULTS

Asymptotic behavior of Vertical Travel-time Sensitivity Kernels (VTSKs)

In a range-independent ocean acoustic waveguide with sound-speed profile $c(z)$, a pulse emitted by a source at depth z_s will travel to a receiver at range r and depth z_r over a multitude of paths and arrive at different times τ_ℓ depending on the path it has traveled along. The vertical travel-time sensitivity kernel (VTSK) $D_\ell(z)$ expresses the sensitivity of arrival time τ_ℓ to perturbations Δc of the sound-speed profile: $\Delta t_\ell = \int_0^H D_\ell(z)\,\Delta c(z)\,dz$. Closed-form expressions for wave-theoretic VTSKs have been obtained from the perturbation of the range-independent Green's function [1] and numerical study has revealed convergence towards the corresponding ray-theoretic VTSKs with increasing range even at low frequencies. In the present work the asymptotic form of finite-frequency kernels with increasing range is derived by applying a stationary-phase approach [2]. The final asymptotic result reads

$$D_\ell(z) = -\frac{1}{r_W b_\ell c^3(z)}\left\{(\dot{u}_\ell - i\dot{w}_\ell)\frac{i}{4p}\sum_{m=1}^{M}\frac{\hat{w}_m^2 \hat{S}_m \hat{j}_m^2(z)\hat{j}_m^2(z_s)\hat{j}_m^2(z_r)}{\hat{k}_m^{3/2}\sqrt{\left|d^2\hat{k}_m/dw^2\right|}}e^{-i\hat{k}_m r + i\hat{w}_m t_\ell - i(a_m+1)\frac{p}{4}}\right.$$
$$\left. -(u_\ell - iw_\ell)\frac{1}{4p}\sum_{m=1}^{M}\frac{\hat{w}_m^3 \hat{S}_m \hat{j}_m^2(z)\hat{j}_m^2(z_s)\hat{j}_m^2(z_r)}{\hat{k}_m^{3/2}\sqrt{\left|d^2\hat{k}_m/dw^2\right|}}e^{-i\hat{k}_m r + i\hat{w}_m t_\ell - i(a_m+1)\frac{p}{4}}\right\}$$

In the above expression k_m and $j_m(z)$ are the real eigenvalues and corresponding eigenfunctions of the vertical Sturm-Liouville problem [3], depending on the circular frequency ω, u_ℓ and w_ℓ are the real and imaginary parts of the complex pressure at the receiver in the time domain evaluated at time τ_ℓ (dots denote time derivatives), $S(\omega)$ is the source signal in the frequency domain, ρ_W the water density, $\Re$ denotes the real part of a complex quantity, and $b_\ell = \dot{u}_\ell^2 + u_\ell\ddot{u}_\ell + \dot{w}_\ell^2 + w_\ell\ddot{w}_\ell$. A hat

marks quantities evaluated at the stationary circular frequency $\hat{\omega}_m$, defined by the equation $dk_m(\hat{\omega}_m)/d\omega = \tau_\ell / r$. Further, δ_m is the sign of $dk_m^2/d\omega^2$ evaluated at $\hat{\omega}_m$.

The following results refer to two different environments, one with a temperate sound-speed profile typical for the North Pacific Ocean, water depth 5400 m, axial depth 1100 m and source/receiver at axial depth, and one with a linear sound-speed profile typical for the Mediterranean Sea in winter, water depth 2500 m and source/receiver at 150-m depth, as shown in Fig. 1. In both cases the bottom is considered absorbing. The propagating acoustic signal is assumed to be a Gaussian pulse with central frequency 100 Hz and 3-dB-bandwidth 50 Hz, unless otherwise mentioned. Normal-mode calculations in the frequency domain, underlying the wave-theoretic as well as the asymptotic VTSK calculations, have been conducted in the frequency range from 5 to 195 Hz.

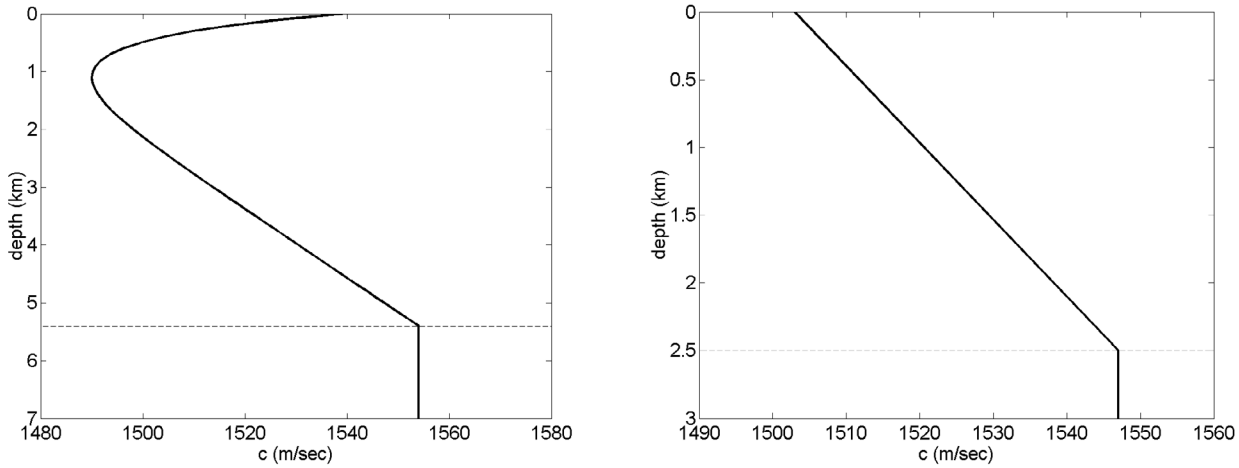

Fig. 1. Typical North Pacific (left) and Mediterranean (right) sound-speed profiles.

Fig. 2 shows the normalized VTSK in the North-Pacific environment for arrivals with the same upper and lower turning depth 315 and 2704 m, respectively, at various ranges, 50, 200, 800 and 1600 km (corresponding to 1, 4, 16 and 32 double loops, respectively). Normalized here means divided by the source-receiver range r; the VTSK, considered as marginal of the corresponding 3D TSK with respect to the horizontal, is proportional to range – thus, division by r results supresses range scaling. It is seen from this figure that the wave-theoretic, long-range asymptotic VTSK (stationary-phase approximation) lies very close to the ray-theoretic VTSK independently of range. This suggests that the ray-theoretic kernel can be seen either as high-frequency or as long-range asymptotic. The wave-theoretic VTSK at 50 km lies close to its asymptotic form at the upper turning depth but exhibits large deviations around the lower turning depth, extending by about 500 m deeper than the corresponding asymptotic and ray-theoretic VTSK. With increasing range these deviations become smaller and finally at 1600 km there is nearly a perfect match even in the details between the wave-theoretic VTSK and its long-range asymptotic.

Fig. 3 shows the normalized VTSKs in the Mediterranean environment for arrivals with the same lower turning depth 1611 m, at ranges 33.3, 100, 300 and 900 km (corresponding to 1, 3, 9 and 27 double loops, respectively). The sound-speed profile is upward refracting in this case, so all propagation paths are surface-reflected. It is seen from this figure that again the wave-theoretic, long-range asymptotic

VTSK lies very close to the ray-theoretic VTSK at all ranges, and so it happens with the wave-theoretic VTSK in the upper 500 m as well, away from the lower turning point. At larger depths deviations occur, and they are largest about the turning depth at 33.3 km range, similar to the North-Pacific case. These deviations become smaller with increasing range. At 900 km there is a perfect match between the wave-theoretic VTSK and its long-range asymptotic.

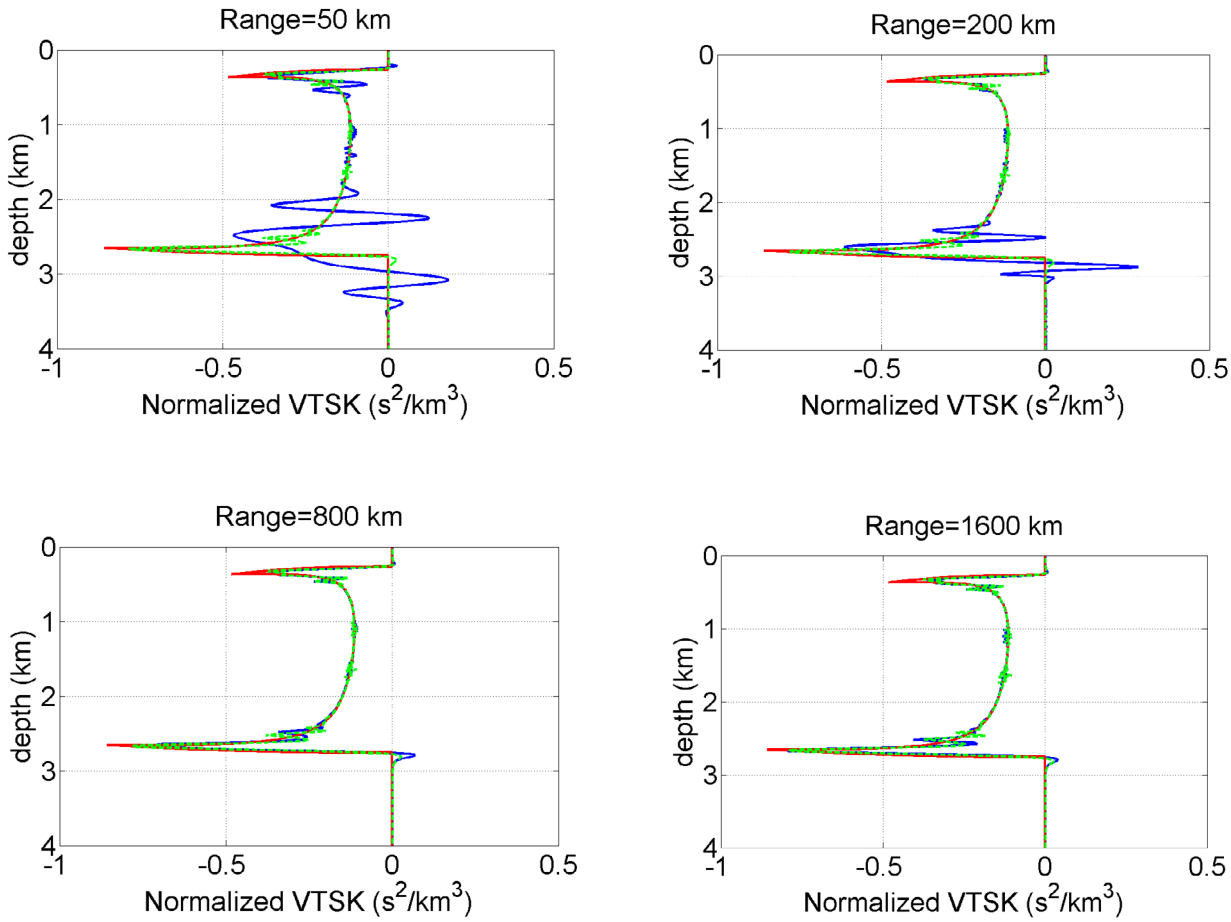

Fig. 2. Normalized VTSKs for North-Pacific profile at various ranges from ray-theoretic (——), wave-theoretic (——) and wave-theoretic asymptotic approach (- - - -).

In the North-Pacific case the apparent difference in the sound-speed profile between the upper and the lower turning depth that might be associated with the different behaviour of the VTSK is the sound-speed rate of change with depth, much higher at the upper than at the lower turning depth. To study this as a possible cause, two bilinear sound speed profiles (Fig. 4) are considered with low and high rate of change, respectively, water depth 3000 m and axis at 1500 m; both source and receiver are assumed at axial depth. Fig. 5 shows the VTSKs for two arrivals with the same upper and lower turning depths, 836 and 2164 m, respectively, and similar propagation range, 56.5 and 56.7 km, respectively, corresponding to 1 and 2 double loops. The difference in the degree of convergence is clear to see. In

the highly refractive case (right hand panel) there is almost perfect agreement whereas in the case of low refraction there are large disagreements both in the amplitude and the support of the kernel. Thus the sound-speed rate of change with depth appears to be a decicive factor in the convergence of the wave theoretic kernel towards the ray-theoretic one at short and medium ranges. At long ranges the connvergence is imposed by the asymptotic behavior, as seen before.

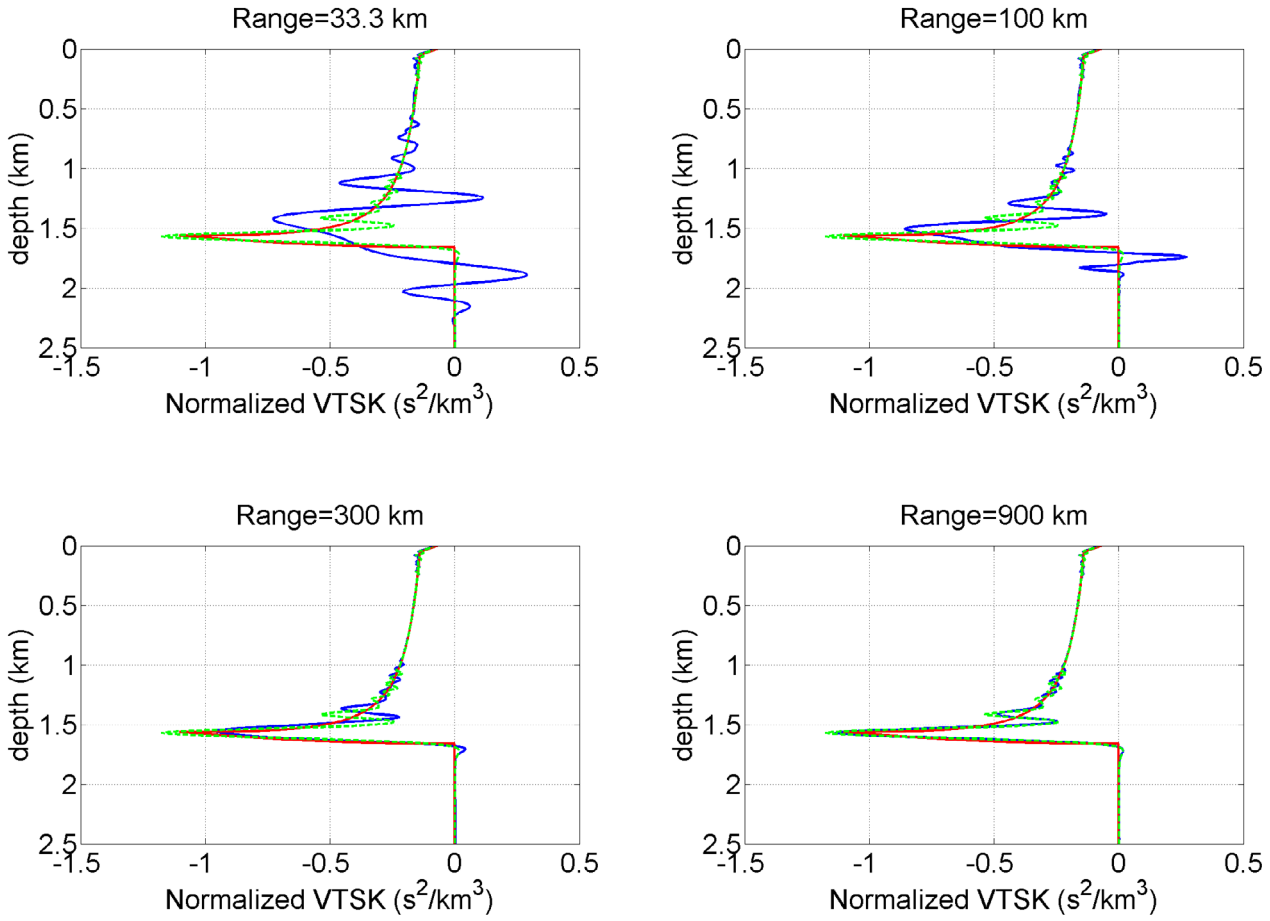

Fig. 3. Normalized VTSKs for Mediterranean profile at various ranges from ray-theoretic (——), wave-theoretic (——) and wave-theoretic asymptotic approach (- - - -).

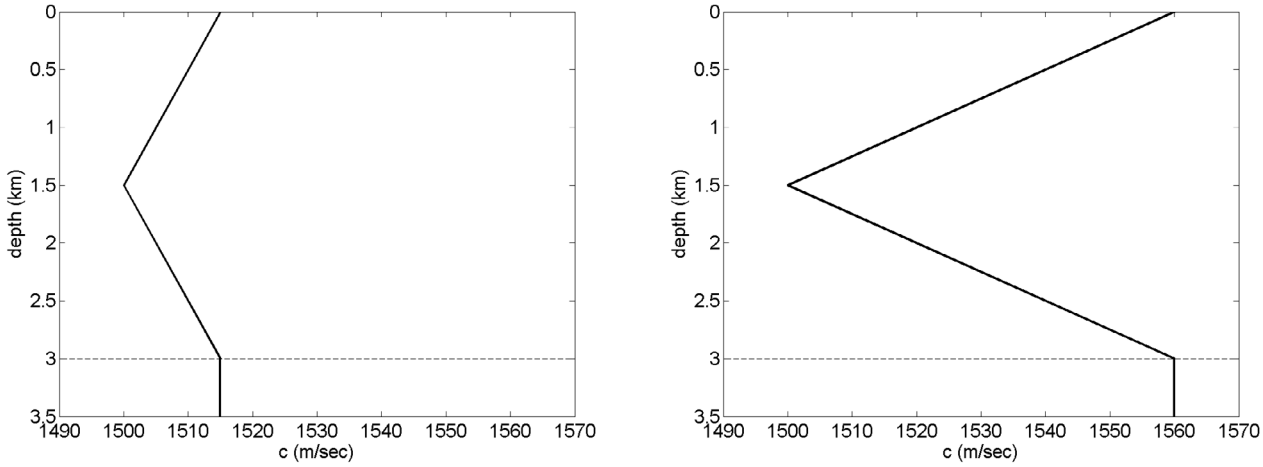

Fig. 4. Bilinear sound speed profiles.

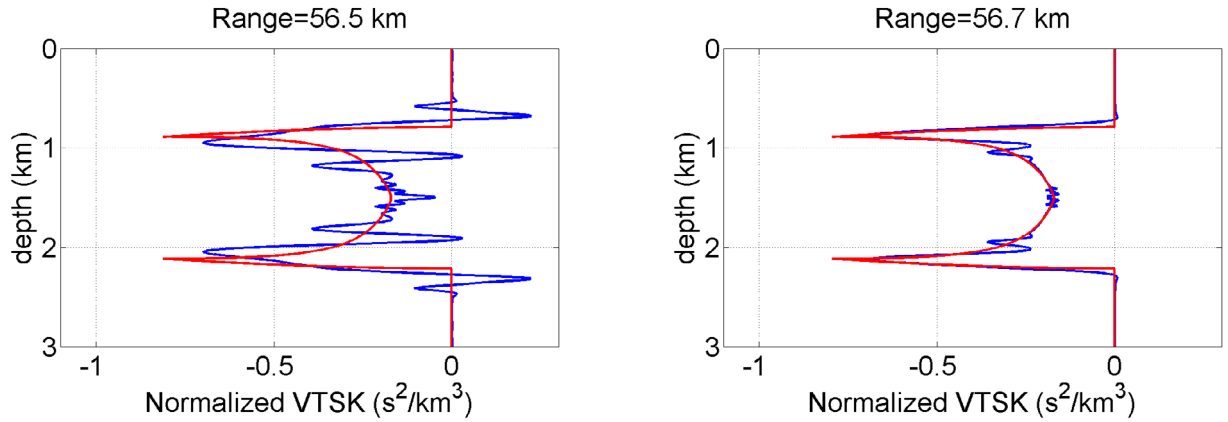

Fig. 5. Normalized VTSKs for bilinear profiles from ray-theoretic (——) and wave-theoretic approach (——).

Sensitivity kernels for arrival amplitudes

Fig. 6 shows a scematic diagram of a pressure arrival as a function of time and how it is perturbed due to a sound-speed change, from c to $c+\delta c$.

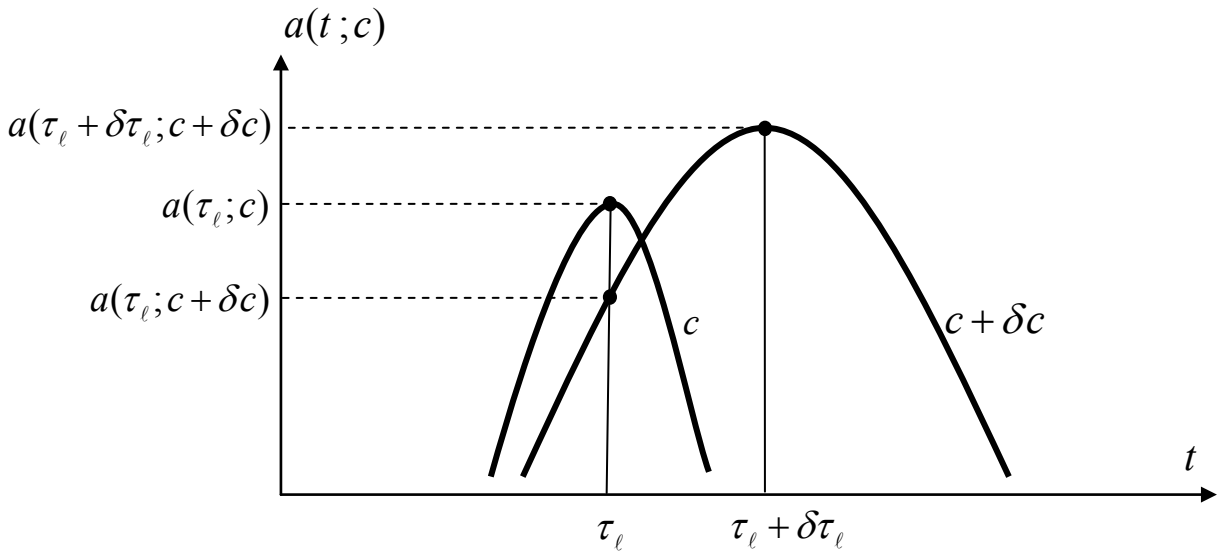

Fig. 6. Definition of arrival amplitude perturbation.

A perturbation δc of the sound speed in general displaces the arrival maximum by $\delta\tau_\ell$ and also changes its amplitude from $a(\tau_\ell, c)$ to $a(\tau_\ell + \delta\tau_\ell, c+\delta c)$. We define two kinds of amplitude perturbations: (i) change of amplitude at fixed time: $\delta a_\ell = a(\tau_\ell, c+\delta c) - a(\tau_\ell, c)$ and (ii) change of maximum amplitude: $\Delta a_\ell = a(\tau_\ell + \delta\tau_\ell, c+\delta c) - a(\tau_\ell, c)$. The resulting first-order perturbation relation turn out to be the same for both definitions, whereas they are slightly different in the second order.

Fig. 7 shows the first-order amplitude sensitivity kernels for three early arrivals in the Mediterranean environment for source-receiver range 33.3 km, using the 3D and the 2D Green's function (left and right panel in Fig. 7, respectively). The signal bandwidth (3dB) in this calculation is 70 Hz.

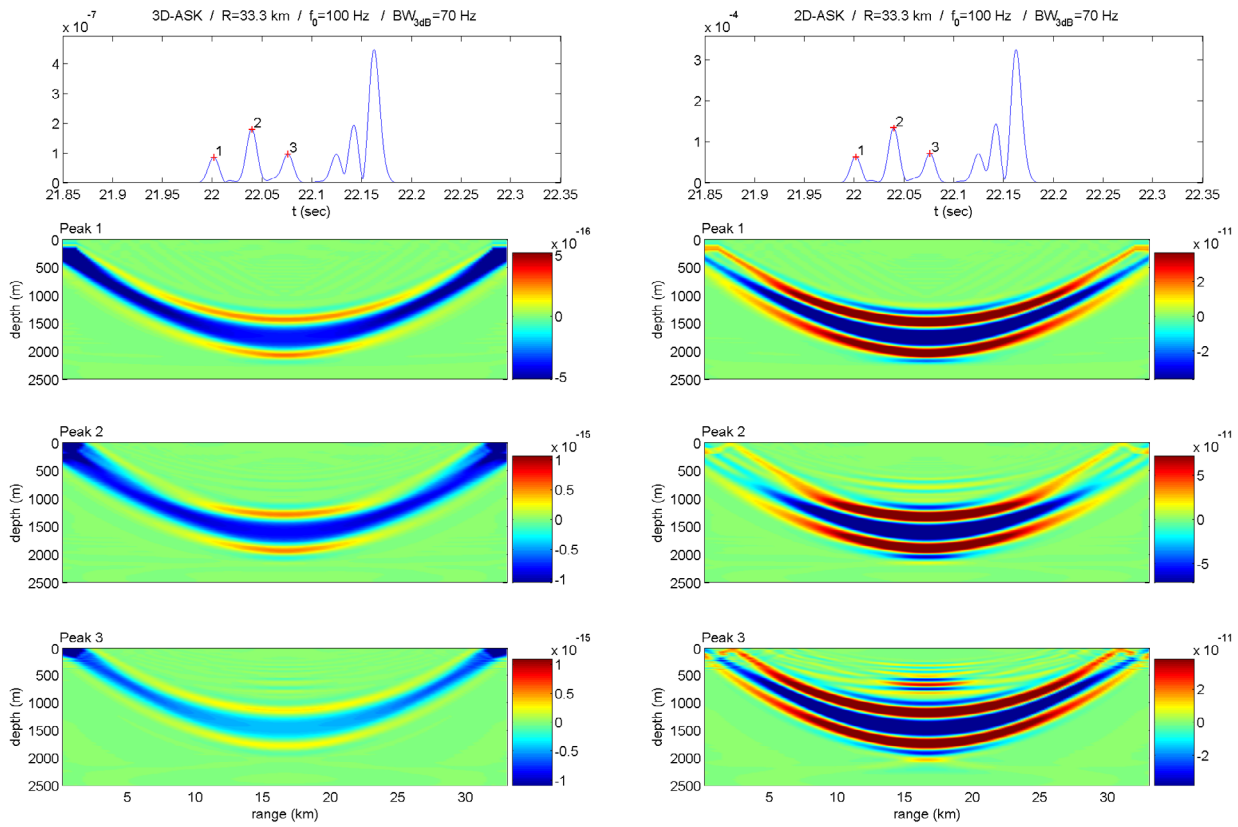

Fig. 7. 3D (left) and 2D (right) arrival pattern and amplitude sensitivity kernels of marked 3 peaks, for propagation range 33.3 km in the Mediterranean environment.

The 2D and 3D arrival patterns (top panels) are similar in shape. The differences in magnitude go back to differences between the 2D and 3D Green's functions [1]. The amplitude sensitivity kernels shown in the lower panels concentrate about the corresponding eigenrays. Each 3D kernel exhibits a broad negative central region (Fig. 7 shows a section of these kernels in the vertical source/receiver plain) followed by weak positive sensitivity areas. The 2D kernels on the other hand exhibit narrower areas of negative sensitivity at the center followed by areas of positive sensitivity at a distance, presenting a more alternating behavior. Fig. 8 repeats the 3D arrival pattern and shows the horizontal cross-range marginals of the 3D amplitude sensitivity kernels (left panels in Fig. 7). The shape similarity between these marginals and the corresponding 2D kernels is remarkable and points to the relation between the two approaches (2D and 3D). The differences in sensitivity magnitude, of similar order as for the arrival patterns) are attributed to differences between 2D and 3D Green's functions.

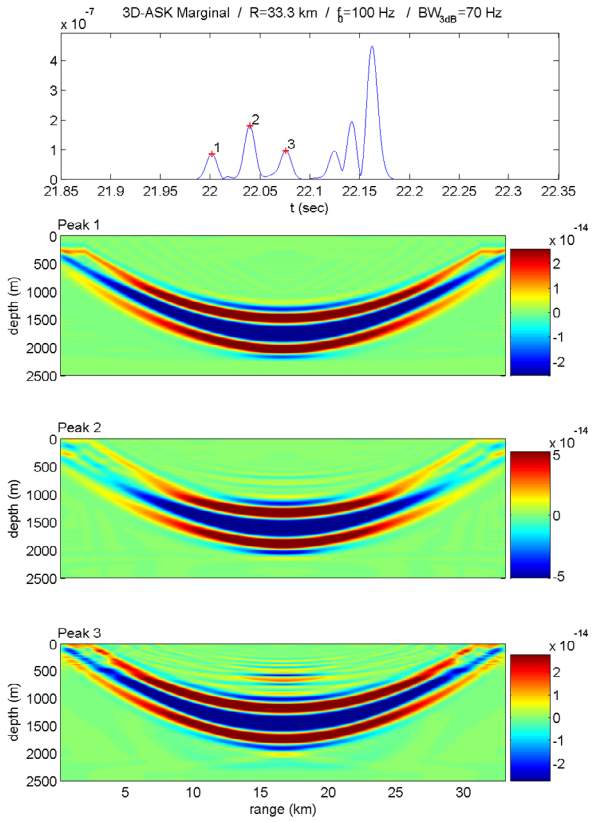

Fig. 8. 3D arrival pattern and horizontal cross-range marginals of 3D amplitude sensitivity kernels of marked 3 peaks, for propagation range 33.3 km in the Mediterranean environment.

In the following some results for first- and second-order vertical amplitude sensitivity kernels (VASKs) are presented. Fig. 9 shows arrival patterns and VASKs, first-order and second-order, for 3 selected peaks in the two different cases, that of maximum amplitude perturbation (right) and that of fixed-time amplitude perturbation (left). The sound-speed profile is the linear Mediterranean profile of Fig. 1, the source/receiver distance 600 km and the 3-dB bandwidth 60 Hz. The first-order VASKs are identical for the two definitions of amplitude perturbation. Each kernel is supported in the neighborhood of the corresponding turning depth and exhibit alternating behavior with a profound negative maximum in the middle. The second-order kernels are also concentrated about the corresponding turning depths, still they are characterized by prevailing negative sensitivity in both cases indicating amplitude reduction as a second-order effect. The second-order sensitivity for amplitude perturbations at fixed time is larger than for maximum amplitude perturbations.

To check these predictions, a comparison with actual behavior of arrival amplitudes is carried out. Fig. 10 shows such a comparison for arrival #1 of Fig. 9. The sound-speed perturbations considered are centered about the turning depth (2055 m) with a vertical extent 100 m and span ±0.3 m/sec. The upper panel in Fig. 10 presents the normalized arrival pattern with the selected peak, whereas the lower panel

shows the actual amplitude (crosses) and the first- and second-order predictions (solid and dashed lines, respectively). The panels on the left refer to amplitude perturbations at fixed time (the background peak arrival time) and those on the right refer to perturbation of the arrival maximum (peak to peak). From these figures it is seen that the actual perturbations exhibit significant deviations from quadratic behavior. In the vicinity of the background state the second-order expansion (dashed line) describes the local curvature, still it cannot describe the full non-linear character. In this connection the second-order ASKs can be useful as an indicator for non-linearity rather than as a tool for inversions.

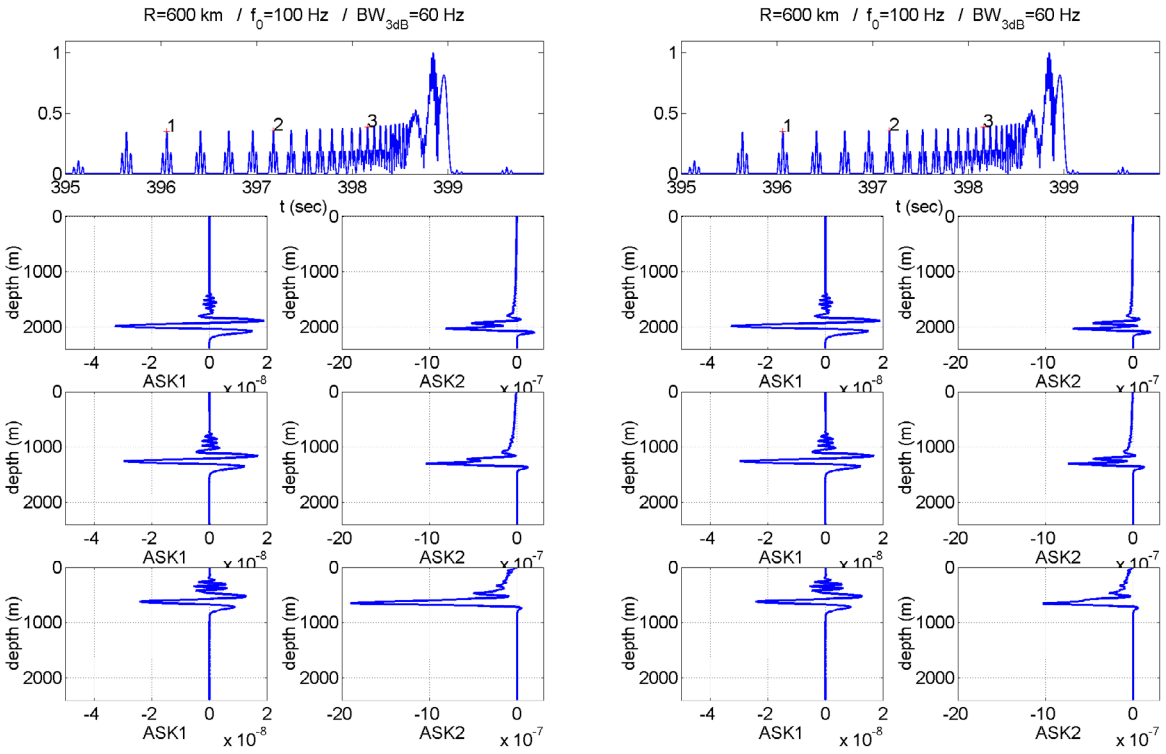

Fig. 9. Arrival pattern and VASKs, first- and second-order of marked 3 peaks, for the fixed-time (left) and maximum (right) amplitude perturbation, in the Mediterranean environment.

IMPACT/APPLICATIONS

The completed work shows that the convergence of wave-theoretic VTSKs towards the corresponding ray-theoretic VTSKs can be rigorously explained by calculating long-range asymptotics using the stationary-phase approach. These asymptotics lie close to the ray-theoretic VTSK even at low frequencies. The conditions governing the application of the stationary phase approximation [4] can be used as an indicator for the convergence behavior of the wave-theoretic kernels.

Coming to amplitude sensitivity kernels, alternative definitions of amplitude perturbations (maximum amplitude, fixed-time amplitude perturbation) have a slight effect on second-order and no effect on first-order perturbations. First-order amplitude sensitivity kernels in 2 and 3 dimensions have similar

shapes to corresponding travel-time sensitivity kernels (TSKs), centered about the respective eigenrays, still lacking a zero-sensitivity core. The horizontal cross-range marginal of the 3D ASK has strong similarities to the corresponding 2D kernel. First- and second-order VASKs have been calculated reproducing the actual perturbation behavior of arrival amplitudes in the vicinity of the background state and can be used as a indicator of non-linearity.

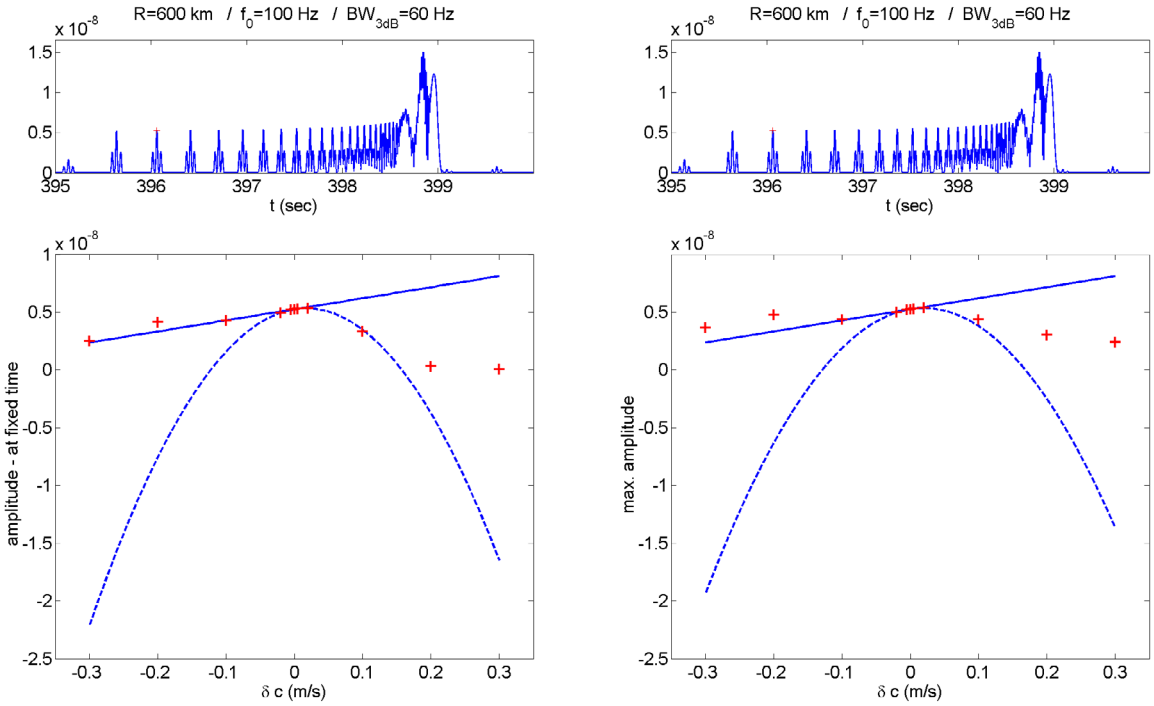

Fig. 10. Arrival pattern and comparison of actual amplitude perturbations of marked peak with first- and second-order predictions, for fixed-time (left) and max. (right) amplitude perturbations.

RELATED PROJECTS

In the framework of NPAL (ONR contract N000140310182) Bruce Cornuelle and Matthew Dzieciuch have been exploring the spatial frequency content and the stability of TSKs in range-dependent ocean environments which produce strong sensitivity of ray paths to initial conditions.

REFERENCES

[1] E.K. Skarsoulis, B.D. Cornuelle, M.A. Dzieciuch, Travel-time sensitivity kernels in long-range propagation, *Journal of the Acoustical Society of America*, Vol. 126, pp. 2223-2233, 2009.

[2] E.W. Erdelyi, *Asymptotic expansions*, Dover, New York, 1956.

[3] F.B. Jensen, W.A. Kuperman, M.B. Porter and H. Schmidt, *Computational Ocean Acoustics*, AIP Press & Springer, New York, 2000.

[4] G.N. Makrakis, E.K. Skarsoulis, Asymptotic approximation of ocean-acoustic pulse propagation in the time domain, *Journal of Computational Acoustics,* Vol. 12, pp. 197-216, 2004.

PUBLICATIONS

E.K. Skarsoulis, B.D. Cornuelle, M.A. Dzieciuch, Second-order sensitivity of acoustic travel times to sound-speed perturbations, *Acta Acoustica*, Vol. 97, pp. 533-543, 2011.